Exploring Phenomena in Nonlinear Dynamical Systems

by

Avina Kalle

A thesis submitted in partial fulfilment of the requirements of BSc. Honours

Azim Premji University

Bengaluru, India

Submitted: June 2020

Abstract

The ubiquity of nonlinear interactions has resulted in the emergence of nonlinear science as an interdisciplinary field over the past several decades. With the advent of modern computers around 1960's, research in nonlinear dynamical systems has become more accessible. Several major developments in the field have been reported in scientific literature (Lakshmanan 2005).
In this work, using computer simulations and other techniques, I explore dynamics in various nonlinear systems which span across the fields of electronics, mechanics, mathematics and epidemiology.

A Chua circuit was constructed on a Printed Circuit Board (PCB) and its behaviour was observed on an analog oscilloscope. It was also simulated using LT-Spice to obtain the corresponding orbits. A dimensionless version of the Ordinary Differential Equations (ODE) system was used to generate its bifurcation diagram using Julia. As expected, there were noticeable differences in the results due to accuracy of the simulation software, imperfections in the physical model and idealisations in the ODE system.

For a mechanical system, the simple elastic pendulum was chosen. Using Lagrange mechanics, the ODEs describing the system were obtained and solved using Julia. For the physical system, Tracker (software) was used to plot its trajectory. As the mathematical model did not consider dissipative forces; even though there was a general similarity, there is a considerable amount of noise that was seen in the physical system.

Julia sets and the Mandelbrot set connect nonlinear systems to complex analysis and fractal geometry. The role of the sets in the orbit of the map $z \mapsto z^2 + c$ were explored using the generation of the sets and the bifurcation diagram. The fractal nature of the sets is explored by computing its dimension and observing self-similarity in the structure.

Finally, a biological model capturing the progression of a disease through a population is investigated. The simple S-I-R ODE model was briefly discussed and a new stochastic cellular automaton is proposed and simulated using 'R'. The drawbacks of the model: lack of some factors, stationary cells, etc. are discussed to suggest improvements.

Through the study of these examples, this project demonstrates key aspects of nonlinear science such as casting problems in terms of ODEs, types of orbits (such as fixed points, periodic and bounded orbits), bifurcation diagrams, iterative maps, stochastic models and cellular automata.

Acknowledgements

Firstly, I would like to acknowledge and thank the university's physics department for the opportunity and help in completing this project.

Secondly, I would like to express my gratitude to my primary research mentor, Kaustubh Manchanda PhD., for her support and guidance.

Last of all, I would like to thank my parents for their constant encouragement. I also thank Manoja, Shantha Bhushan PhD. and Kripa Gowrishankar PhD. for their support and motivation throughout the project.

Table of Contents

List of Tables

List of Figures

Chapter 1 Introduction

Nonlinear systems are present everywhere around us and are encountered in different disciplines (Lakshmanan 2005). Despite the ubiquity of the nonlinear phenomenon, we tend to simplify and idealize systems to a simple, analytically solvable and straight forward form wherein the non-linear terms are negligible and are ignored. This approximation gives accurate results most of the time (small-angle approximations in optics, finding trends using linear regression models, etc.); it is easily understood, visualized and developed on. However, certain systems have high non-linear dependencies which cannot be eliminated and thus finding an analytical/closed-form solution for such systems is a challenge (such as the classical mechanics three-body problem (Musielak and Quarles 2014)). Some of these systems are the focus of my study, in this project.

Chapter 2 Materials and Methods

The subtopics explored in this project were studied through

i. Experiments
ii. Theoretical readings
iii. Simulations: LT-Spice was used for the electronic systems and R for Cellular Automata models
iv. Numerical solutions: Programming language 'Julia'

Chapter 3 Chua Circuit

Chua circuit is one of the basic types of nonlinear circuit capable of showing chaos. It has been extensively studied, since its invention in 1983 by Leon O. Chua (Matsumoto 1984). The beauty in this circuit lies in its easy construction, well-defined outputs and easily available and detailed prior academic work (by Leon O. Chua), making it an ideal starting point for investigating the field of nonlinear dynamics.

3.1. **Nonlinear Circuits**

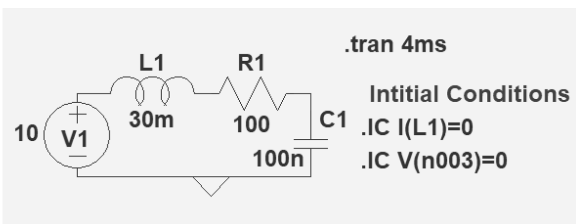

Figure 3-1: RLC circuit schematic, with LT spice code

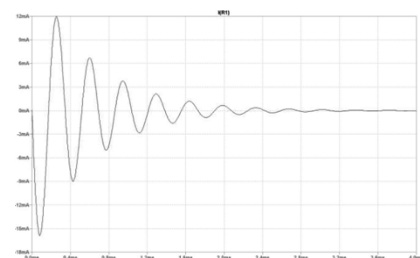

Figure 3-2: RLC Simulation (I vs. t)

One of the simplest nonlinear circuits is the RLC circuit (**Figure 3-1**), where the energy in the circuit flips from the inductor to the capacitor and back again. However, the resistor dissipates energy and over time there is no current flowing through the circuit (**Figure 3-2**). If one considers the phase plot of this system: I_L (current flowing through the inductor) vs. V_c (voltage across the capacitor), when R is changed from a negative value to positive through 0, qualitatively different orbits are observed (**Figure 3-3**).

Figure 3-3: RLC circuit orbit: I_L vs. V_C

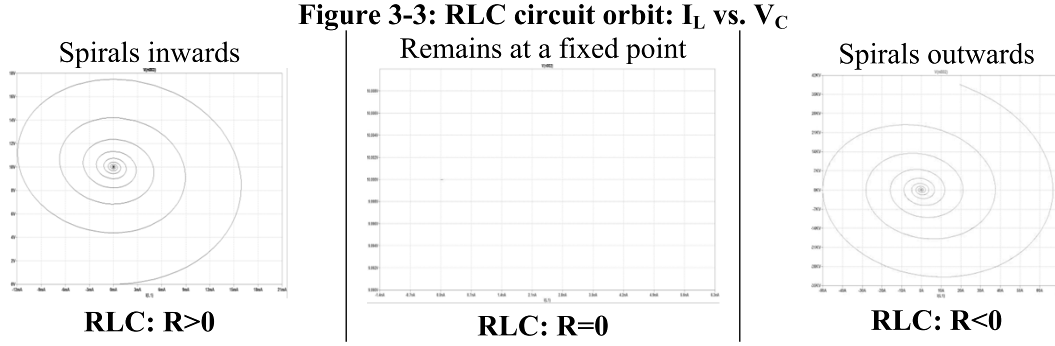

3.2. **Chua diode**

A Chua diode is a negative resistor whose resistance depends on the voltage applied across it. The typical I-V characteristics of such a diode are shown in **Figure 3-4** and are described by **Equation 3-1**.

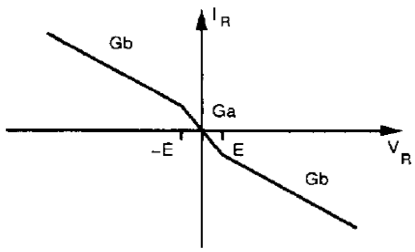

Figure 3-4: Typical Chua diode characteristics (Kennedy 1993)

Equation 3-1: Chua diode i-v characteristics

$$g(V_R) = I_R = \begin{cases} G_b V_R + E(G_b - G_a) & if \quad V_R < (-E) \\ G_a V_R & if \quad V_R \in [-E, E] \\ G_b V_R - E(G_b - G_a) & if \quad V_R > E \end{cases}$$

This was simulated in LT-Spice as shown in **Figure 3-5**.

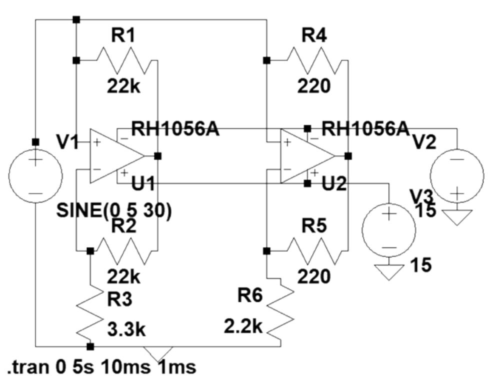

Figure 3-5: LT-Spice schematic Chua diode

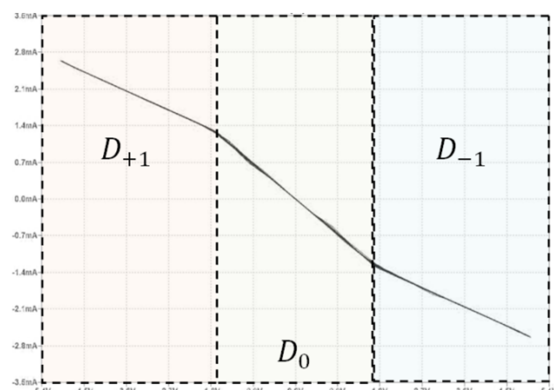

Figure 3-6: LT-Spice Simulated i-v characteristics

The data points, in **Figure 3-6**, were analyzed using MS Excel to get the following quantities:

$E = 1.7V$

$G_a = -7.54 \times 10^{-4} \Omega^{-1}$

$G_a = -4.1 \times 10^{-4} \Omega^{-1}$

3.3. **Chua Circuit**

A Chua circuit is a type of parallel RLC circuit, whose basic outline is as shown in **Figure 3-7**.

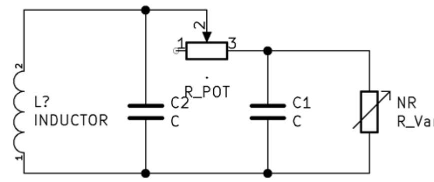

Figure 3-7: Outline of Chua Circuit

3.3.1. **Mathematical Analysis**

This system is non-linear due to the presence of a diode which has a three-piece linear behaviour and its overall behaviour can be concisely described by **Equation 3-2**.

Equation 3-2: Ordinary Differential Equation (ODE) system of the Chua's circuit

$$\begin{bmatrix} \dot{V}_1 \\ \dot{V}_2 \\ \dot{i}_L \end{bmatrix} = \begin{bmatrix} G/C_1 & -G/C_1 & 0 \\ G/C_2 & -G/C_2 & 1/C_2 \\ 0 & -1/L & 0 \end{bmatrix} \begin{bmatrix} V_1 \\ V_2 \\ i_L \end{bmatrix} + \begin{bmatrix} g(V_1) \\ 0 \\ 0 \end{bmatrix} where, \begin{matrix} V_1 = & voltage\ across\ C_1 \\ V_2 = & voltage\ across\ C_2 \\ i_L = & current\ through\ L \\ G = & conductance\ of\ R_{POT} \end{matrix}$$

3.3.2. **Dimensional Analysis**

The system can also be defined as in **Equation 3-3** (Sood, Abhirakshit and Shiva 2014).

Equation 3-3: Dimensionless form of Chua's circuit

$$\begin{bmatrix} \dot{x} \\ \dot{y} \\ \dot{z} \end{bmatrix} = \begin{bmatrix} 0 & \alpha & 0 \\ 1 & -1 & 1 \\ 0 & -\beta & 0 \end{bmatrix} \begin{bmatrix} x \\ y \\ z \end{bmatrix} - \alpha \begin{bmatrix} h(x) \\ 0 \\ 0 \end{bmatrix} \quad \text{where} \quad \begin{matrix} x = \frac{V_1}{E_1} & y = \frac{V_2}{E_1} & z = \frac{Ri_L}{E_1} \\ \tau = \frac{t}{RC_2} & a = G_a R & b = G_b R \\ \alpha = \frac{C_2}{C_1} & \beta = \frac{R^2 C_2}{L} & \end{matrix}$$

3.4. **Simulations**

3.4.1. **LT-Spice Simulation**

The circuit in **Figure 3-8** was simulated in LT-Spice XVII, a plotting software 'Plotly' was used to generate 3-D graphs from the data of the simulation and Excel was used to find the periodicity of different periodic orbits.

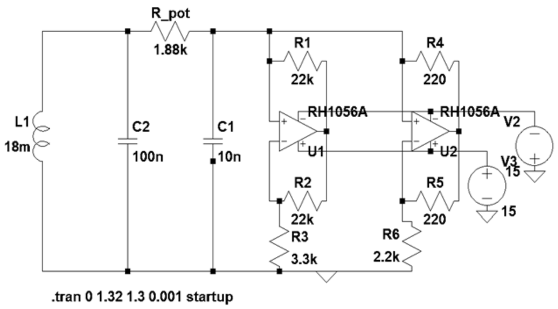

Figure 3-8: LT-Spice schematic of Chua circuit, with program line

Table 3-1: Periodicity of orbits

R_pot (Ω)	Time period (s)	Periodicity
2000	0.00034	1
1950	0.00067	2
1944.5	0.001	3
1860	0.0034	10

Figure 3-9: Various types of periodic orbits in Chua circuit

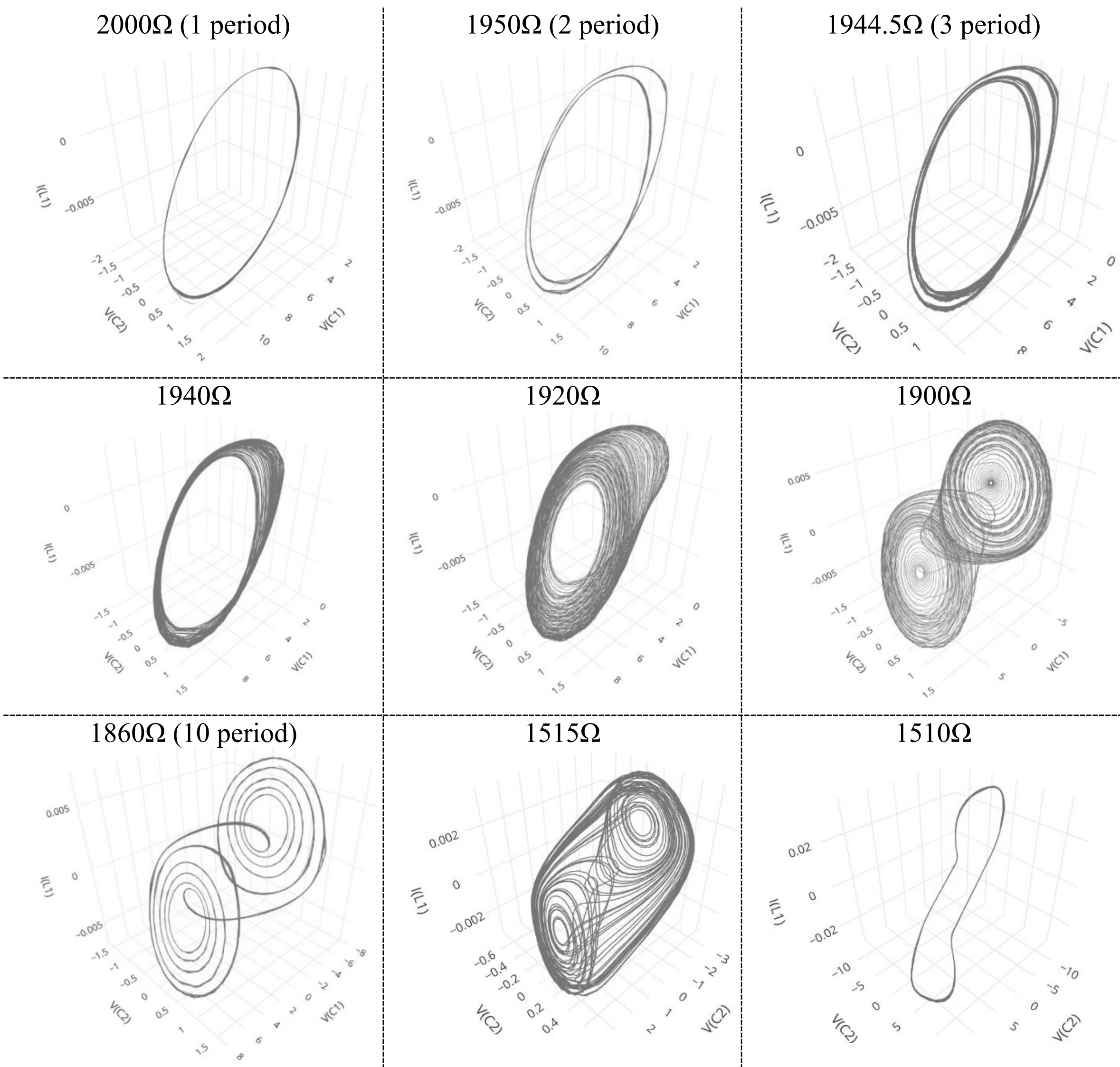

3.4.2. **Bifurcation diagram of the Dimensionless form of the Chua Circuit**

The script in **Code 1** was used to generate the bifurcation diagram of the ODE system in **Equation 3-3** for different values of resistance of the potentiometer.

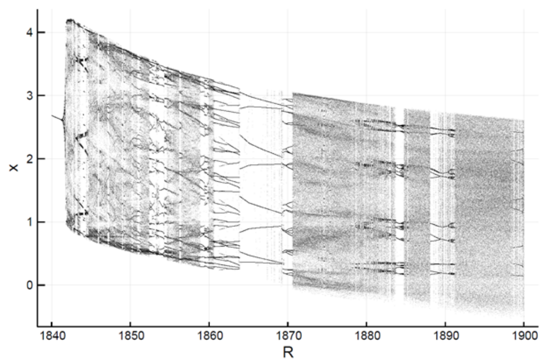

Figure 3-10: Bifurcation diagram x vs. R

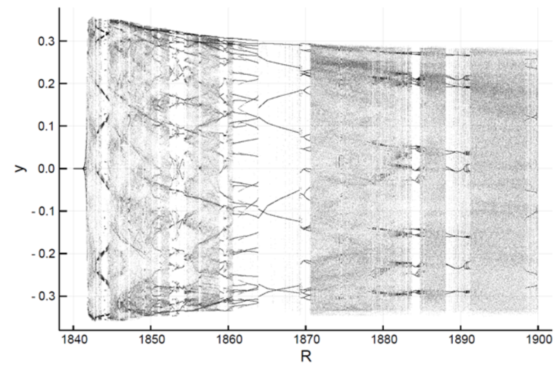

Figure 3-11: Bifurcation diagram y vs. R

Deviations are observed in these orbits as compared to those obtained from the LT-Spice Simulation (in **Figure 3-9**). This could be because LT-Spice offers a more realistic simulation of the actual circuit by factoring in the resistance of the inductor, internal characteristics of the IC from an ideal op-amp, etc.

3.4.3. **Physical Experiment**

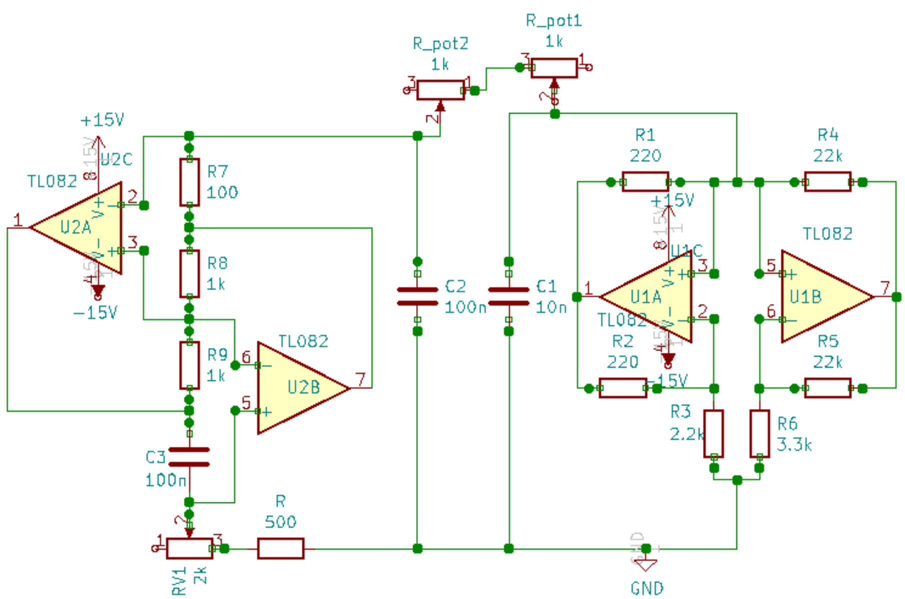

Figure 3-12: Schematic for physical Chua Circuit

3.4.3.1. **Results Obtained**

1.986kΩ

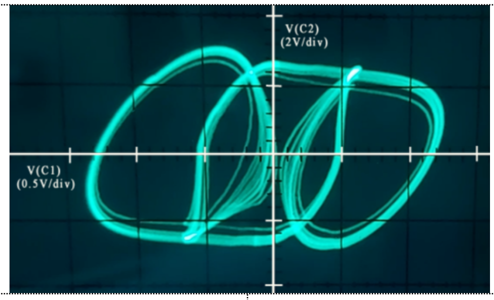

1.976kΩ

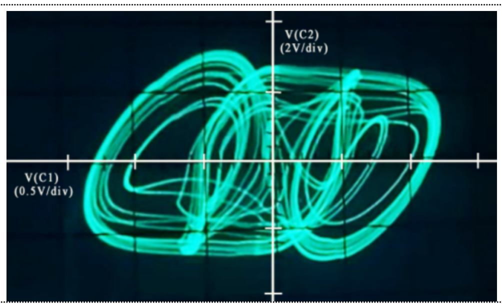

1.913kΩ

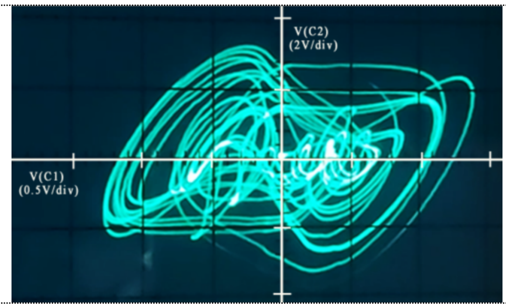

1.8625kΩ

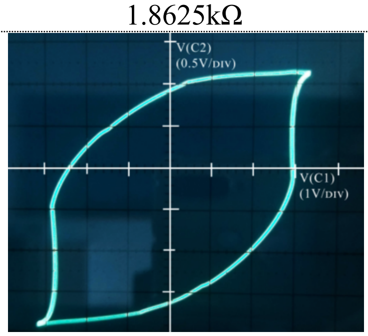

1.389kΩ

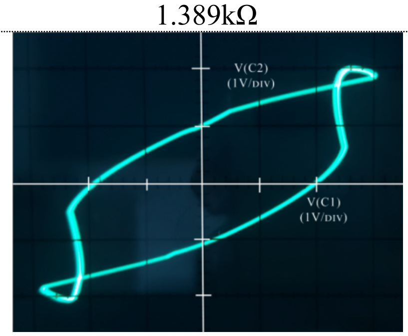

Figure 3-13: Orbit of Chua Circuit (Analog Oscilloscope)

3.5. **Discussion**

The Chua circuit is a simple and easy to implement, non-linear and chaotic analog circuit. The limitations of the theoretical model can be seen through the LT-spice simulation and the physical circuit. This system can be coupled with a slave circuit to demonstrate synchronisation.

A proposed practical application for such a circuit is encryption. A signal is combined with the output signal of the circuit and then decrypted with an “inverse” circuit. Here, one can think of the “key” for decryption to be the parameter set. (Mulukutla and Aissi 2002)

Chapter 4 Elastic Pendulum

An elastic pendulum is a simple pendulum whose string can be modelled as a spring.

4.1. **Mathematical Expression for Motion**

Position of bob = (x,y)

Natural length = l_0 ;   Extension = s

Angle with (0,y) = θ; Spring constant = k

Natural frequency $\coloneqq \omega_s = \sqrt{\frac{k}{m}}$

Kinetic energy= $T = \frac{1}{2}mv^2 = \frac{1}{2}m \cdot \left(\dot{x}^2 + \dot{y}^2 + \dot{z}^2\right)^{\frac{1}{2}}$

Potential energy = $V = V_{gravity} + V_{spring} = -mgy + \frac{1}{2}k\left(l_0 - \left(x^2 + y^2 + z^2\right)^{\frac{1}{2}}\right)^2$

Lagrange: $\mathcal{L} = T - V = \frac{1}{2}m \cdot \left(\dot{x}^2 + \dot{y}^2 + \dot{z}^2\right)^{\frac{1}{2}} + mgy - \frac{1}{2}k\left(l_0 - \left(x^2 + y^2 + z^2\right)^{\frac{1}{2}}\right)^2$

$$\frac{\partial}{\partial x}\mathcal{L} = -\frac{1}{2}k \cdot 2\left(l_0 - \left(x^2 + y^2 + z^2\right)^{\frac{1}{2}}\right) \cdot \left(-\frac{1}{2}\left(x^2 + y^2 + z^2\right)^{-\frac{1}{2}} \cdot 2x\right)$$

$$= k \cdot x \cdot \left(\frac{l_0}{\left(x^2 + y^2 + z^2\right)^{\frac{1}{2}}} - 1\right)$$

Lagrange set of equations: $\frac{d}{dt}\frac{\partial}{\partial \dot{x}}\mathcal{L} = m\ddot{X}$

Equation 1: $m\ddot{x} = k \cdot x \cdot \left(\frac{l_0}{\left(x^2 + y^2 + z^2\right)^{\frac{1}{2}}} - 1\right)$

$$\Longrightarrow \ddot{x} = \frac{k}{m} \cdot x \cdot \left(\frac{l_0}{\left(x^2 + y^2 + z^2\right)^{\frac{1}{2}}} - 1\right)$$

Similarly, $\ddot{y} = \frac{k}{m} \cdot y \cdot \left(\frac{l_0}{\left(x^2 + y^2 + z^2\right)^{\frac{1}{2}}} - 1\right) - g$ and $\ddot{z} = \frac{k}{m} \cdot z \cdot \left(\frac{l_0}{\left(x^2 + y^2 + z^2\right)^{\frac{1}{2}}} - 1\right)$

4.2. **Julia Simulation**

4.2.1. **Code**

The system described above was simulated using Julia-1.1.1: **Code 2**

4.2.2. **Results**

Figure 4-1: Simulated elastic pendulum

4.3. **Physical Experiment**

An elastic pendulum was constructed using a spring, weights and a stand. The software "Tracker" was used to track the motion of bob and the trajectory was found.

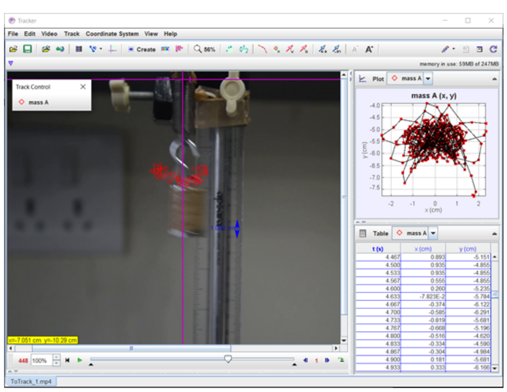

Figure 4-2: Tracker software to find the trajectory of an elastic pendulum

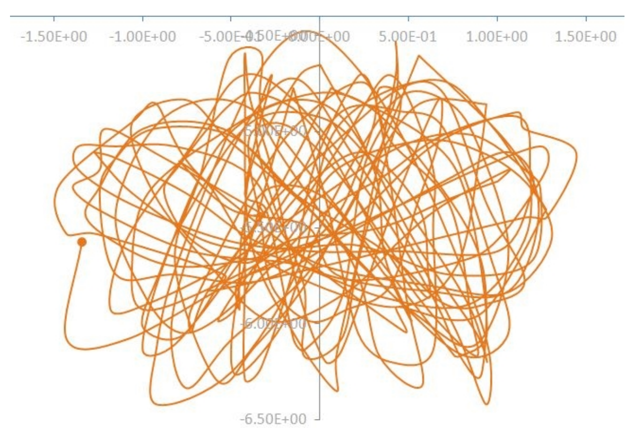

Figure 4-3: Obtained trajectory of elastic pendulum

4.4. **Results and Discussion**

Comparing **Figure 4-1** and **Figure 4-3**, one can find that there is some qualitative similarity between the two in terms of the overall inverted bean-like shape that the trajectory covers. However, one can also see that the simulated trajectory looks smoother and intuitively not realistic. This can be accounted for by the fact that the mathematical model did not take into account the following factors:

i. Friction between the spring and stand
ii. Internal friction of the spring (dissipated energy)
iii. Slight movements of the stand (the stand was stuck, at the top, to a cupboard to make it stable; but this still did not make it completely stable)
iv. The bob is approximated to be a point mass

Including all these factors is beyond the scope of this project and was not done. Nonetheless, one can conclude that an elastic pendulum is an interesting example that can be economically and easily constructed in a lab setting and can be used to demonstrate the effect of how oversimplification of a system can result in visible disparities.

Chapter 5 Julia Sets and the Mandelbrot Set

Polynomials are simplest functional forms which can be studied; in particular, those with degree 2, namely quadratics; i.e, g:$z \to az^2 + bz + d$ where $x, a, b, c \in \mathbb{F}$ (field) have interesting applications (a classic example being projectile motion). If this field is taken to be the complex numbers, it is trivial to prove that there is a homomorphism between g and f: $z \to z^2 + c$ such that $g(z) = \phi^{-1}(f(\phi(z)))$ $\forall z \in \mathbb{C}$, where $c = ad + \frac{b}{2} - \left(\frac{b}{2}\right)^2$ and $\phi(z) = az + \frac{b}{2}$. If one needed to study the iteration of g, it would suffice to study that of f since $g^n = \phi^{-1} \circ f^n \circ \phi$ where p^n denotes the n$^{\text{th}}$ iterate of p.

Julia sets were first described by Gaston Julia in the 1918, after he returned from World War I without his nose. The Mandelbrot Set was studied by Benoit B. Mandelbrot around the late 20$^{\text{th}}$ century, resulting in the revival of Julia sets. It can be thought of as the parameter space of f and has an equally complex and intricate structure.

5.1. **Definition**

5.1.1. **Julia Set**

A filled Julia set $\mathcal{K}(f, c)$, defined on a polynomial f:$z \to z^2 + c$, are those $z \in \mathbb{C}$ for which the orbit of $f^n(z)$ remains bounded $\forall n \in \mathbb{N}$, where $f^0(z) = z$ and $c \in \mathbb{C}$ is a constant. The Julia set $\mathcal{J}(f,c)$ is the boundary of the filled Julia set $\mathcal{K}(f, c)$.

5.1.2. **The Mandelbrot Set**

The Mandelbrot set is the set of all $c \in \mathbb{C}$ for which the orbit of $f^n(0)$ remains bounded under iteration.

$$\mathcal{M}(f) \stackrel{\text{def}}{=} \left\{c \in \mathbb{C} : \left|f^n(0)\right| \leq 2, \forall n \in \mathbb{N} \;\&\; f{:}z \to z^2 + c\right\}$$

Equivalently, the Mandelbrot set is the set of all values of $c \in \mathbb{C}$ whose Julia set $J(f,c)$ is connected.

5.2. **Generating Julia Sets and the Mandelbrot Set**

Code 3 and **Code 4** was used to generate the Mandelbrot set and Julia sets.

5.2.1. **The Mandelbrot Set**

Code 3 generates **Figure 5-1** and by changing the centre and extent of the frame, one can “zoom” into the set and observe the intricacies within, as shown in **Video 1**[1] that zooms in towards the point -0.244-0.756i, revealing smaller quasi similar Mandelbrot sets.

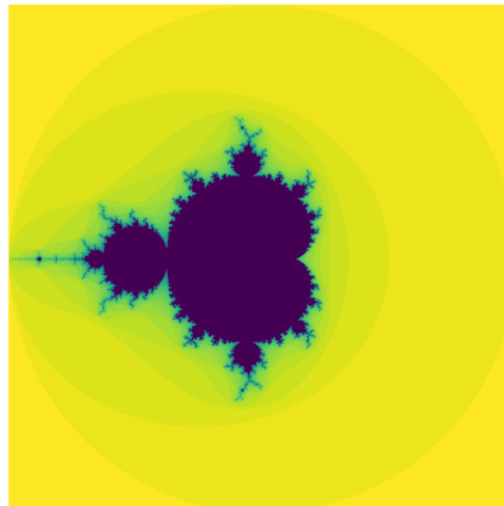

Figure 5-1: The Mandelbrot Set

5.2.2. **Julia Sets**

The **Code 4** was used to generate Julia Sets along the real line, by changing c.

Figure 5-2: Julia Sets along the real line

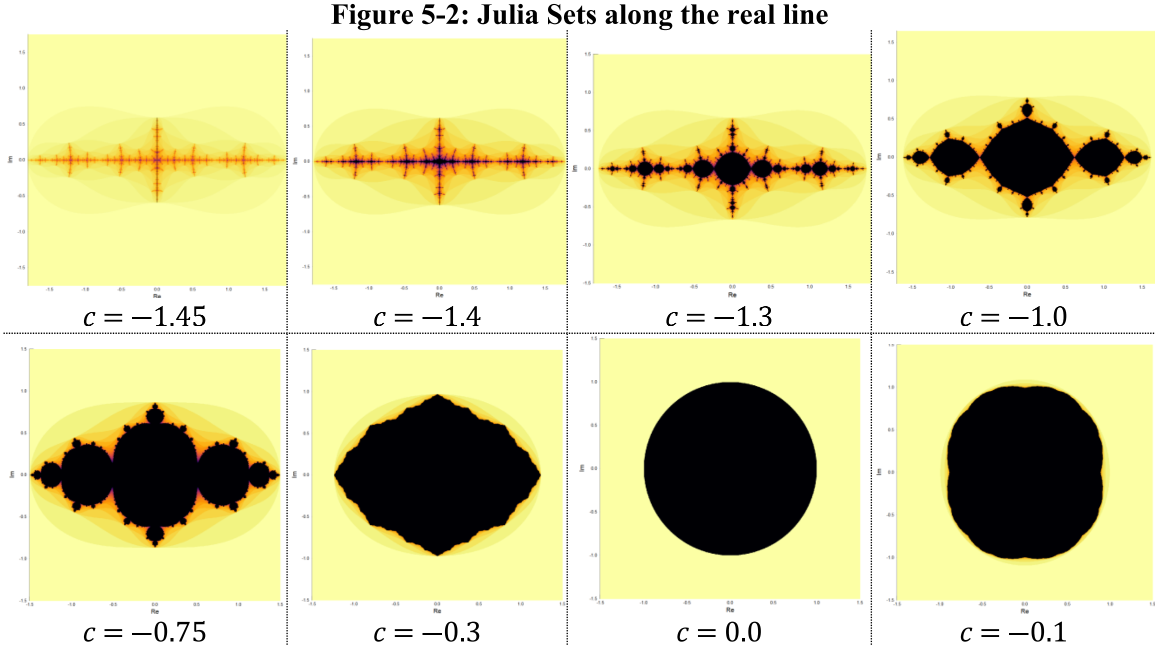

[1] https://github.com/Avina-cK/NLD_Julia/blob/master/MandelbrotSet/ZoomSequences/SelfSimilarZoomSequence_-0_243922_-0_7560655.gif

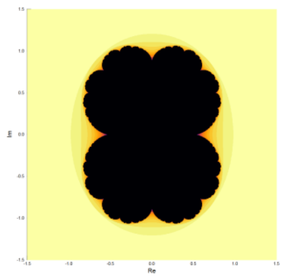

$c = 0.25$

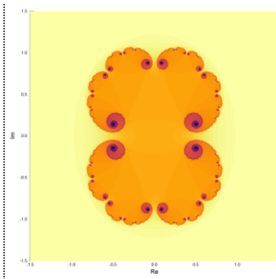

$c - 0.27$

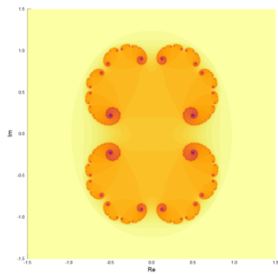

$c = 0.3$

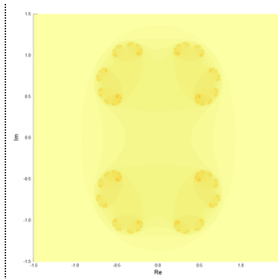

$c = 0.5$

5.3. **Observations and Inferences**

5.3.1. **Fractal nature**

5.3.1.1. **Understanding fractals**

Before looking into what a fractal is and how it connects to these sets, a few pre-requisite definitions shall be stated.

Topological space: $(X, \mathcal{T})$

X is a set. $\mathcal{T} = \{U_i\}: U_i \subseteq X$ such that:

i. X and $\emptyset$ are open sets.

ii. $U_i \in \mathcal{T}: \bigcup U_i$ is open.

iii. $U_i \in \mathcal{T}: \bigcap_{i=1}^{k} (U_i)$ is open, $k \in [1,\infty)$

$\mathcal{T}$ is a topology on X. $(X, \mathcal{T})$ is a topological space.

δ –cover of a topological space

$\{U_i\}: \forall i, U_i \subseteq X$. The diameter of a set $U_i := D_{U_i} = \sup\{|x - y| : x,y \in U_i\}$.

$\delta := \sup\{D_{U_i} : U_i \in \{U_i\}\} > 0$. If $X \subseteq \bigcup(U_i)$, the set $\{U_i\}$ is called the δ-cover of X.

s-dimensional Hausdorff measure of F

For $F \subset \mathbb{R}^n$, the *s-dimensional Hausdorff measure* of F is defined as follows:

$$\mathcal{H}^s(F) = \lim_{\delta \to 0} \inf \left\{ \sum_i |U_i|^s : \{U_i\} \textit{ is a } \delta\textit{-cover of } F \right\}$$

Consider $F \subseteq \mathbb{R}^n : x \in F$. $\mathcal{B}_r(x)$ is an open ball of radius r at x; its boundary is $\mathcal{O}_r(x)$.

Topological dimension

The topological dimension of F is $\dim_{\mathrm{T}} F = k$.

i. $\big(\forall x \in F, \exists r{:}\forall y \in \mathcal{B}_r(x), y \notin F\big) \Rightarrow k = 0$

ii. $\big(\forall x \in F \;\&\; r \in \mathbb{R}, \big(\mathcal{O}_r(x) \cap F\big) = L{:}\dim_{\mathrm{T}}(L) = K - 1\big) \Rightarrow k = \min K$

Hausdorff–Besicovitch dimension[2]

The Hausdorff–Besicovitch dimension of F is $\dim_{\mathrm{H}} F = D(F)$

$$D(F) = \inf\{d \geq 0{:}\mathcal{H}^s(F) = 0\}$$

Fractal[3]

F is a fractal $\Leftrightarrow \dim_{\mathrm{T}} F < \dim_{\mathrm{H}} F$

Box-counting dimension (Minkowski[4]–Bouligand dimension)

The box-counting dimension of $F \subset \mathbb{R}^2$ is $\dim_{\mathrm{MB}} F$. Let $N(l)$ be the number of solid squares of side l required to cover F. Then,

$$\dim_{\mathrm{MB}} F \coloneqq \lim_{l \to 0} \left|\frac{\log\left(N(l)\right)}{\log\left(l\right)}\right|$$

Examples:

i. Square

A square (S) of side 1 can be divided into N smaller squares of side length $\frac{1}{\sqrt{N}}$.

$$\dim_{\mathrm{HB}} S = \left|\frac{\log N}{\log \frac{1}{\sqrt{N}}}\right| = \left|-2\left(\frac{\log N}{\log N}\right)\right| = 2$$

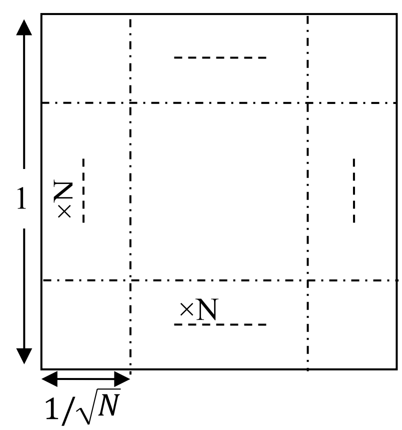

---

[2] For further reading: (DeLorto 2013)

[3] This definition was first given in the book: *The Fractal Geometry of Nature* (Mandelbrot 1982)

[4] Hermann Minkowski is known for developing the concept of Minkowski spacetime that explains and supports Einstein's (who was his student) General Theory of Relativity.

ii. Sierpinski triangle

The Sierpinksi triangle (S_Δ) is a fractal that can be formed through an iterative affine transformation that contains triangles within triangles.

Given that the length of the largest triangle's side is 1, N boxes of side length l are needed to cover it: where $N = 3^n$ and $l = \frac{1}{2^n}$.

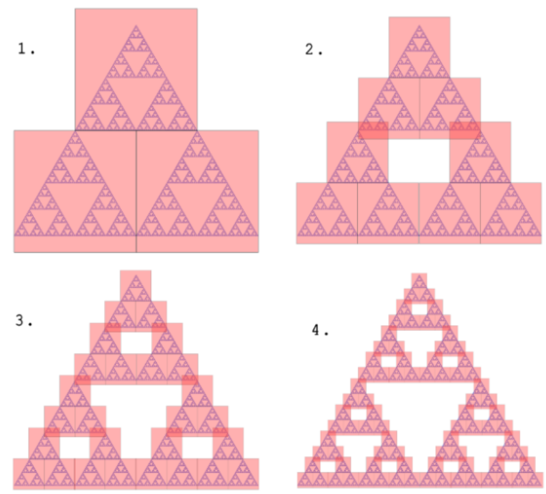

Figure 5-3: Covering the Sierpinski triangle with boxes

$$\dim_{\mathrm{MB}} S_\Delta = \left|\frac{\log 3^n}{\log\left(\frac{1}{2^n}\right)}\right| = \left|\frac{\log 3}{\log 2}\right| = 1.58496\ldots$$

5.3.1.2. **Fractal dimension**

An interesting observation one makes is that no matter how much one zooms into the boundary of $M(f)$ ($\stackrel{\text{def}}{=} \partial M(f)$), there is always some roughness/irregularity (**Video 2**[5]: zoom sequence into i). This leads to $\partial M(f)$ having a Hausdorff dimension of 2 (Shishikura 1998); i.e, $\partial M(f)$ is a fractal.

Not all Julia Sets are fractals, that of $c = 0$ is a circle and is not a fractal; but the further away c is from the Mandelbrot Set, one can see that the Julia sets becomes "dustier"; as seen in **Figure 5-2**.

5.3.1.3. **Self-similarity**

[5] https://github.com/Avina-cK/NLD_Julia/blob/master/MandelbrotSet/ZoomSequences/ZoomSequence_around_i.mp4

Zooming into the intricate boundary of the Mandelbrot set, one can see many interesting and repeating patterns. One can also find tinier versions of the entire set at different scales. These smaller versions are not exactly the whole set, and hence, there is a property of quasi self-similarity in the set.

Some Julia sets have parts that recur in the set, but with a smaller size and at an angle. Shown in **Figure 5-4** is an example of the Julia set of $c = 0.25 + 0.5i$ where the three bulbs repeat on each other, like the budding of a yeast cell.

Figure 5-4: Self similarity in the Julia set of c=0.25+0.5i

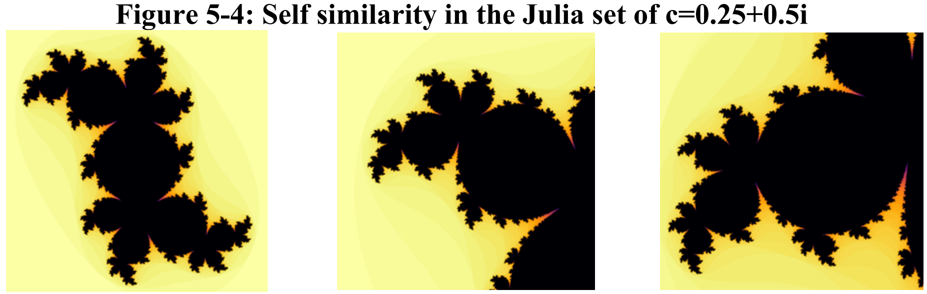

5.3.2. **Periodicity of f(0)**

Different orbital periods of $f^n(0)$ for different values of c correspond to different topological regions in the Mandelbrot Set. Figure 5-5 shows how the orbits change as c changes along the real line.

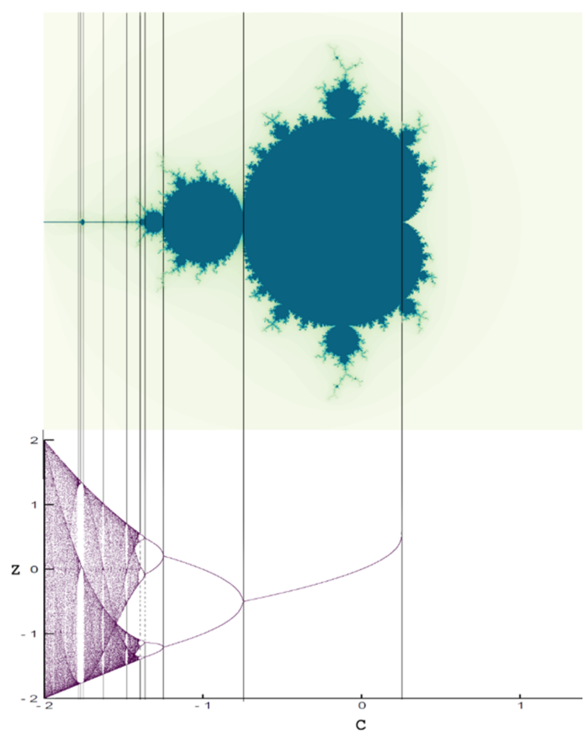

Figure 5-5: Bifurcation diagram of $f^n(0)$ and its corresponding topological areas

An interesting pattern observed is in the period of the orbits that belong to the "bulbs" of the main cardioid: the period is equal to the number of spokes on the bulb. **Table 5-1** shows the periodicity of the orbit starting from the topmost large bulb and moving to the second largest on the right, then the largest between the previous two and so on.

The Julia sets for c in these bulbs also have the same number of "bulbs" (including the main segment) symmetrically on either side of ~(1,1) line.

Table 5-1: Periodic orbits of c in different bulbs of the Mandelbrot set

$\boldsymbol{c}$	**Area in Mandelbrot set**	**Orbit of $\boldsymbol{f(0)}$**	**Filled Julia set $\boldsymbol{\mathcal{K}(f,c)}$**
$-0.12+0.75i$	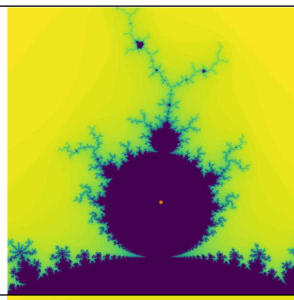	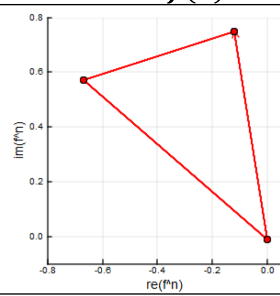	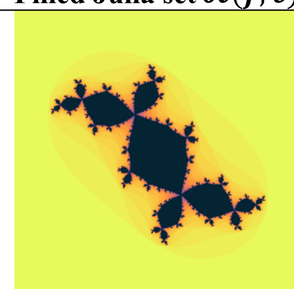
$-0.5+0.55i$	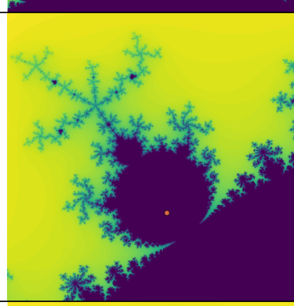	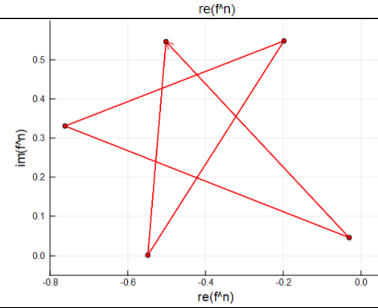	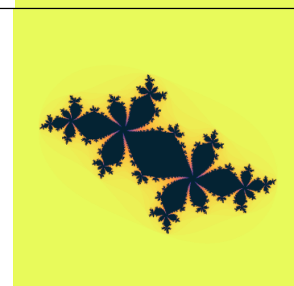
$-0.36+0.615i$	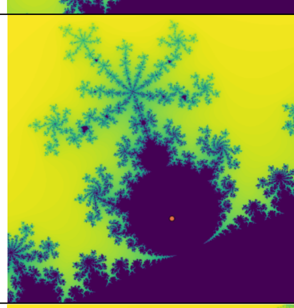	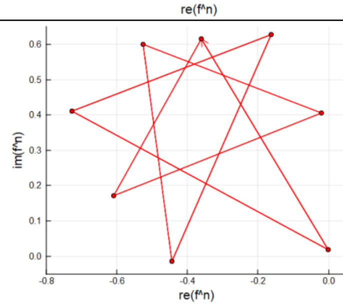	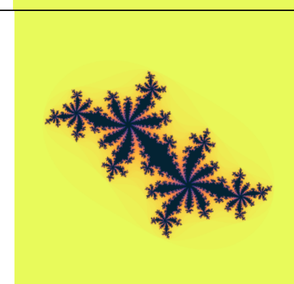
$-0.407+0.585i$	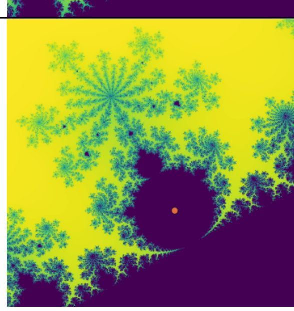	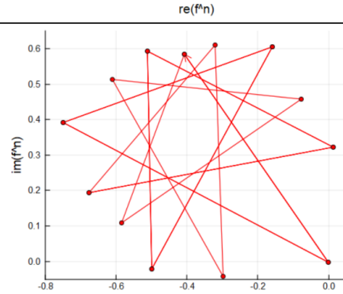	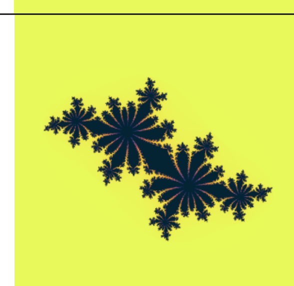

One can easily see that the period of the orbits is as follows: 3, 5, 8, 13; which is the Fibonacci sequence. Now, one obvious question to ask is: does this continue if the same algorithm was used to select bulbs and it turns out that this is true (Devaney 1995)!

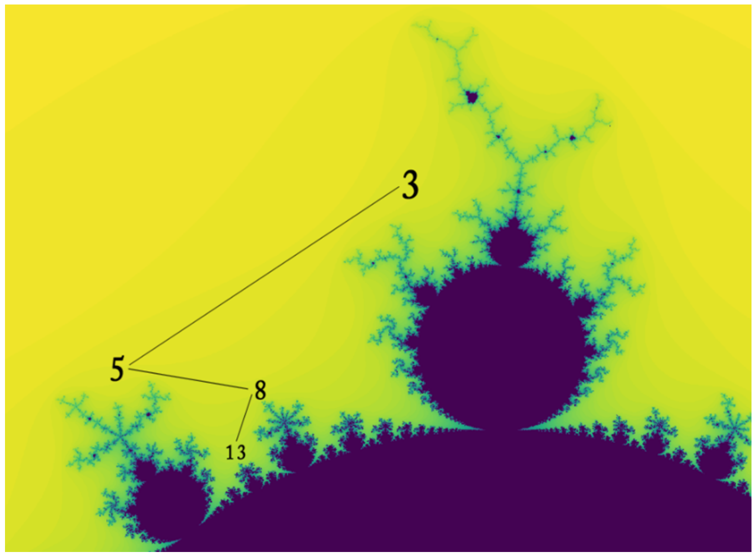

Figure 5-6: Fibonacci sequence in the Mandelbrot set

5.4. **Discussion**

The Julia Sets and the Mandelbrot set are classical examples that arouse interest in nonlinear dynamics and various other fields of mathematics. The emergence of complex behaviour in what seems to be a very simple map: $z \to z^2 + c$ is quite fascinating. The sets themselves have no direct application and are researched and studied purely for fascination and aesthetics.

Figure 5-7: Genesis Effect (yyz1335 2008)

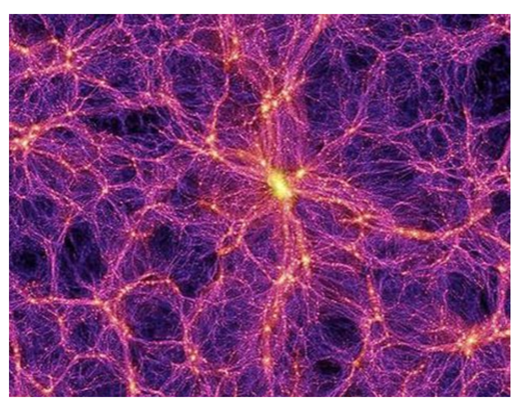

Figure 5-8: Cosmic Web (Springel 2019)

However, the study of fractal geometry has extensive applications in many fields of science (Kluge 2000). The damaged Death Star in *Star Wars: Episode VI – Return of the Jedi* and planet surface, during the Genesis Effect (**Figure 5-7**) in the feature film *Star Trek II: Wrath of Khan* had computer-generated fractal landscapes (IBM n.d.), with the latter being the first of its kind! Fractal analysis is also used to analyse financial markets (Mandelbrot, A Multifractal Walk Down Wall Street 1999), the distribution of galaxies and the cosmic web (**Figure 5-8**), heartbeats and neurological systems (IBM n.d.).

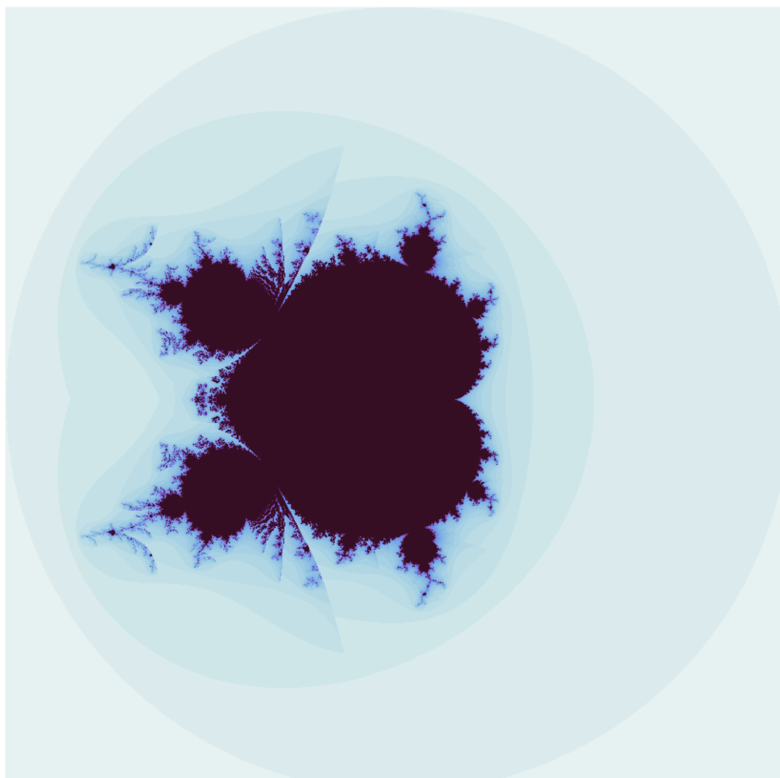

Figure 5-9: Mutlibrot set for d=2.2

One can also explore the Multibrot sets: sets generated using the iterative map $z \to z^d + c$ where $d(\geq 2) \in \mathbb{R}$, which also give interesting fractal structures (the evolution of Multibrot sets as d changes from 2 to 5 is shown in **Video 3**[6]).

[6]https://github.com/Avina-cK/NLD_Julia/blob/master/MultibrotSets/EvolutionOfMultibrots.mp4?raw=true

Chapter 6 Dynamics of Infectious Diseases

Logistic growth system is one of the simplest nonlinear models used extensively to study population growth. This models a simplified system where there are no diseases and no unexpected fluctuations caused by external factors. The following chapter will introduce a model to simulate the evolution of an infection in a population.

6.1. **SIR Model**

For this model, we shall consider the fixed population size ‘N’ which is partitioned into three categories: susceptible (S), infected (I) and resistant (R) (this contains all the people who have either recovered or died due to the disease). The model that governs this system is as follows (Wikipedia n.d.):

Figure 6-1: Schematic of SIR model

Equation 6-1: SIR Model

$$\dot{S} = -\beta\frac{SI}{N}$$

$$\dot{I} = \beta\frac{SI}{N} - \gamma I$$

$$\dot{R} = \gamma I$$

β = probability of getting infected × no. of contacts/ person;

γ = rate of recovery/ death

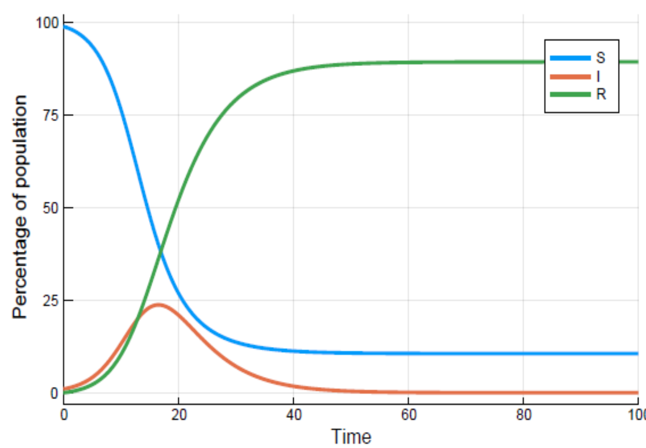

Figure 6-2: SIR time evolution for parameters [0.5, 0.2]

The trajectory that was found above shows a very smooth progression of a population that is infected, like a simplistic isolated system that is quite unrealistic.

6.2. **Modifying the model**

Some factors that can be considered are:

i. Birth rate (b.r)

ii. Death rate (d.r)

iii. Mutation (m.r)

iv. Vaccination (v.r)

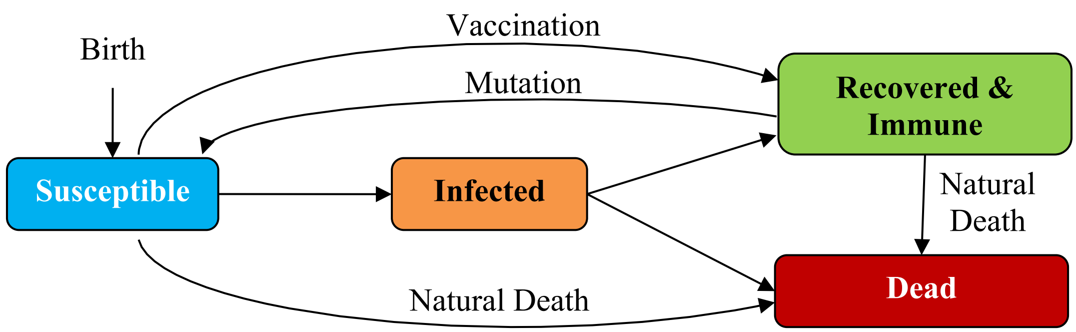

Figure 6-3: Schematic of modified population model

The population is discrete and the time scale at which the infection progresses is in days, which shall be considered as discrete.

6.2.1. **Cellular Automata**

A d-dimensional cellular space is defined to be a subset of $\mathbb{Z}^d$, which contain cells denoted by $\vec{n}$. The state of a cell is given by $c(\vec{n})$.

A cellular automaton (CA) $\mathcal{A}$ is a 4-tuple: (d, S, N, f) where

i. d is the dimensionality of the cellular space

ii. S is the set of states that a cell can be in.

iii. N is a set of the relative neighbours of a cell.

iv. f is the local update rule. This defines the new state of a cell based on the state configuration of its neighbourhood.

6.2.2. **Defining the CA**

A cellular automaton can be written to model the modified system:

$$\mathcal{A} = \left(2, \{0,1,2,3\}, M_1^2, f\right)$$

Where M_1^2 is the Moore neighbourhood of radius 1:=central cell and eight cells around it.

f: $c\left(M_1^2(\vec{n})\right) \rightarrow c'(\vec{n})$

$$P\left(c'(\vec{n}) = 1\right) = \begin{cases} b.r & if \quad c(\vec{n}) = 0 \\ m.r & if \quad c(\vec{n}) = 3 \end{cases}$$

$$P\left(c'(\vec{n}) = 2\right) = i.r \quad if \quad c(\vec{n}) = 1 \wedge 2 \in c\left(M_1^2(\vec{n})\right)$$

$$P\left(c'(\vec{n}) = 3\right) = \begin{cases} v.r & if \quad c(\vec{n}) = 1 \\ r.r & if \quad c(\vec{n}) = 2 \end{cases}$$

$$P\left(c'(\vec{n}) = 0\right) = d.r \quad if \quad c(\vec{n}) = 1,2,3$$

Parameter vector: $[br, rr, dr, ir, mr, vr]$

6.2.3. **Code**

The above system was implemented using the programming language R: **Code 5**[7]**.**

6.2.4. **Results**

6.2.4.1. **Cellular automata visualisation**

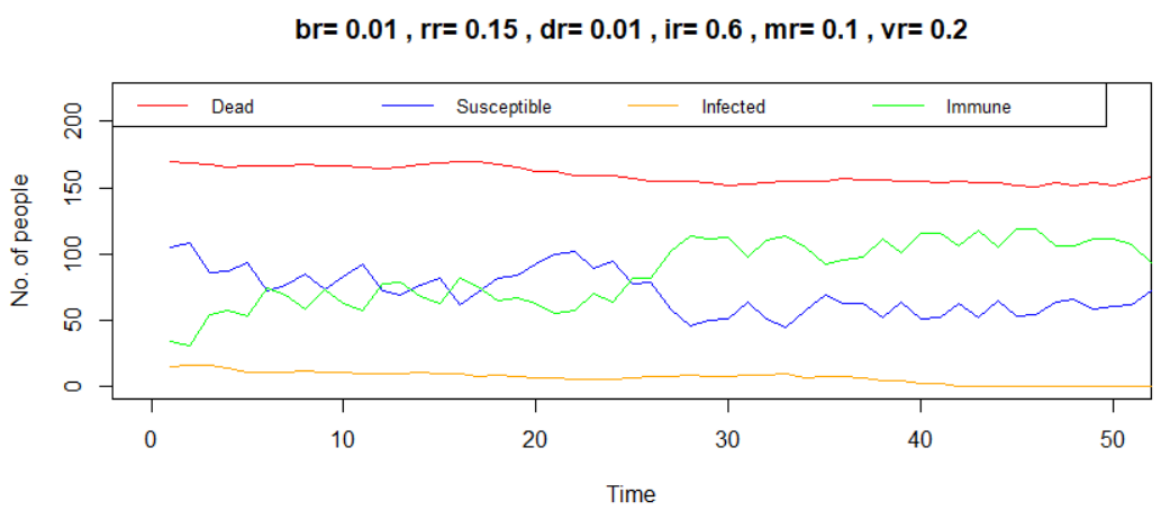

Figure 6-4: Time series plot of an infected population

[7] https://github.com/Avina-cK/CA_InfectiousDiseases/blob/master/CA_InfectionInPopulation.R

Figure 6-5: Evolution of infected population (time step = 10)

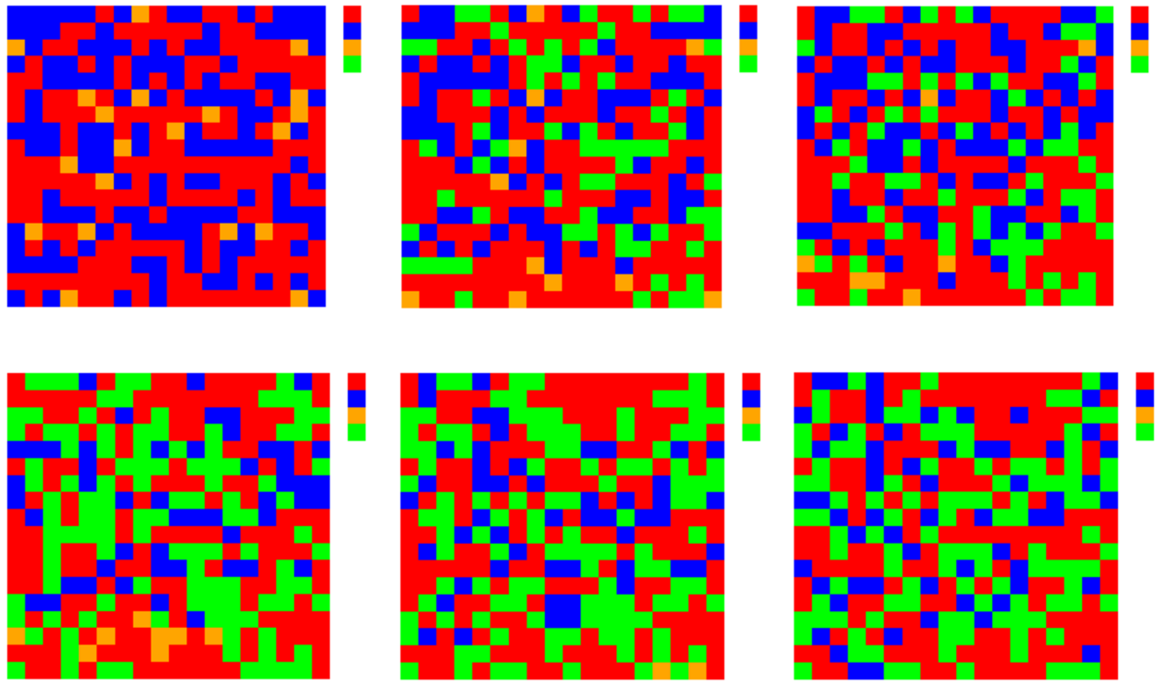

6.2.4.2. **Changing rate of recovery**

Table 6-1: Time Series of Population- r.r: 0.12 → 0.15

r.r.	0.12	0.15
Time Series of population	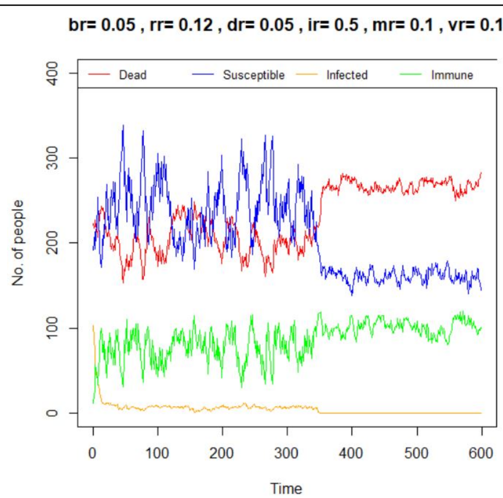	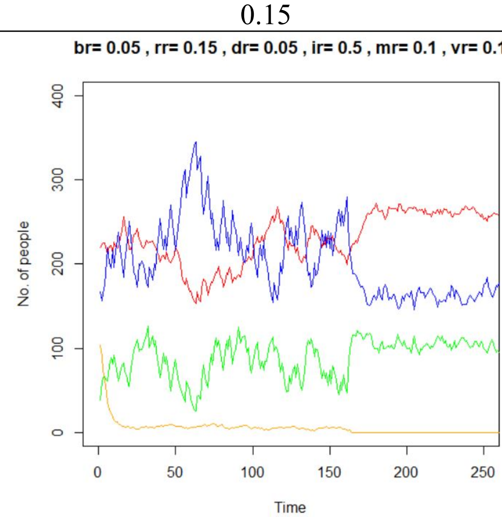

When the recovery rate is increased by 25%, the time taken for total recovery has reduced roughly by 50%, as shown in **Table 6-1**.

6.2.4.3. **Changing infection rate**

Table 6-2: Time Series of Population- i.r: 0.5->0.6

<table>
<tr><th>i.r.</th><th>0.5</th><th>0.6</th></tr>
<tr><td>Time Series of population</td><td>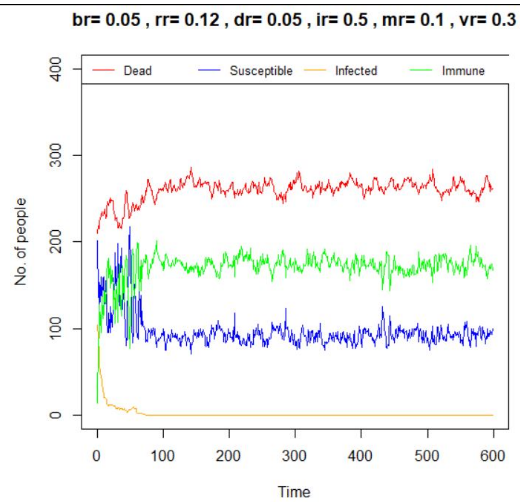
</td><td>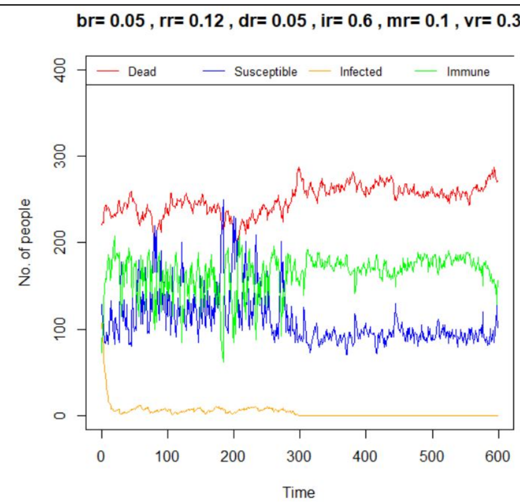
</td></tr>
</table>

When one increases the infection rate, the plots in **Table 6-2** show that the infection takes longer to die down and it takes longer for the population to stabilise.

6.2.5. **Observations and Inferences**

i. The introduction of more factors (vaccination, mutation, death rate and birth rate) and the non-deterministic evolution (i.e, probabilistic evolution) of the state of the population correspond more closely to real-life situations.

   One main aspect that can be distinctly seen in the plots is the noisy progression of the population.

ii. One major drawback of this model is that individuals are stationary and do not move. The movement of individuals is a key factor in determining how a pandemic occurs in different parts of the world; which is why strict immigration rules are put in place during outbreaks.

iii. The only interaction between cells is when one cell infects another. The phenomenon of maternal immunization, the influence of people to make sure/ disallow others to get vaccinated, etc does not exist.

6.3. **Discussion**

Stochastic nonlinear systems have been extensively used to model epidemics. Furthermore, modelling stochastic systems using cellular automata has been a very popular approach owing to the ease of working with CA's. Spatial cellular automata models for infected populations show that the infection spreads geographically and gives a good visual representation of the same (Sayama 2019). It is also easy to keep modifying this model stochastically by adding more conditions. This sort of simulation is realistic and intuitive since population numbers (individuals) is a discrete entity, probabilistic updates occur at each site and changes in the global state take place in discrete time (namely, the number of cases reported/ recovered is updated every day).

The CA model defined in **6.2.2** is a simplistic model that can be further modified by changing the shape of the cellular space, adding factors that simulate movement, changing the neighbourhood of cells, etc. Once enough factors have been taken into consideration, one can also try matching it with previously collected real-life data.

Chapter 7 Conclusion

This project explored several types of dynamical systems, namely Ordinary Differential Equations, Iterative Maps, Stochastic models and Cellular Automata. These can be used as effective starting points for delving into nonlinear dynamics owning to their simplistic nature, ease of realising in a laboratory setting and accessibility of the necessary tools for simulating and numerically solving them.

Code

Code 1: Bifurcation graphs of Chua Circuit
https://github.com/Avina-cK/NLD_Julia/blob/master/Chua_Circuit/ChuaCircuit_BifurcationDiagram.jl

Code 2: Elastic Pendulum
https://github.com/Avina-cK/NLD_Julia/blob/master/Elastic_Pendulum/ElasticPendulum.jl

Code 3: Generating the Mandelbrot set
https://github.com/Avina-cK/NLD_Julia/blob/master/MandelbrotSet/PlottingTheMandelbrotSet.jl

Code 4: Generating Julia sets
https://github.com/Avina-cK/NLD_Julia/blob/master/JuliaSets/PlottingJuliaSets.jl

Code 5: Cellular Automata Model of an infected population
https://github.com/Avina-cK/CA_InfectiousDiseases/blob/master/CA_InfectionInPopulation.R

References

DeLorto, Robert. *Fractal dimension and Julia Sets.* Masters Thesis, EWU Masters Thesis Collection, Eastern Washington University, Cheney: EWU Digital Commons, 2013.

Devaney, Robert L. "The Fractal Geometry of the Mandelbrot Set 2. How to Count and How to Add." *Fractals* (World Scientific Publishing Company) 3, no. 4 (1995): 629-640.

IBM. *Fractal Geometry.* IBM. https://www.ibm.com/ibm/history/ibm100/us/en/icons/fractal/transform/

Kennedy, M. P. "Three steps to Chaos. Part-II: A Chua's Circuit Primer." *IEEE Transactions on Circuits and Systems I: Fundamental Theory and Applications*, 1993: 657-674.

Kennedy, M. P. "Three Steps to Chaos-Part I: Evolution." *IEEE Transactions on Circuits and Systems I: Fundamental Theory and Applications*, 1993: 640-656.

Kluge, Tino. "Fractals in nature and applications." 05 December 2000. https://kluge.in-chemnitz.de/documents/fractal/node2.html (accessed January 15, 2020).

Lakshmanan, M. "Nonlinear dynamics: Challenges and perspectives." *Pramana* (Indian Academy of Sciences) 64, no. 4 (April 2005): 617-632.

Mandelbrot, Benoit B. "A Multifractal Walk Down Wall Street." *Scientific American* (Springer Nature America, Inc.), February 1999: 70-73.

—. *The Fractal Geometry of Nature.* New York: W. H. Freeman and Company, 1982.

Mulukutla, Mahesh, and Cherif Aissi. "Implementation of the Chua's circuit and its applications." *2002 ASEE Gulf-Southwest Annual Conference.* Lafayette: American Society for Engineering Education, 2002. 8.

Musielak, Z. E., and B. Quarles. "The three-body problem." *Reports on Progress in Physics* (IOP Publishing Ltd) 77, no. 6 (June 2014).

Rackauckas, C., and Q Nie. "DifferentialEquations.jl – A Performant and Feature-Rich Ecosystem for Solving Differential Equations in Julia." *Journal of Open Research Software* 5, no. 1 (2017): 15.

Sayama, Hiroki. *Examples of Biological Cellular Automata Models.* 9 Nov 2019. https://math.libretexts.org/Bookshelves/Applied_Mathematics/Book%3A_Introduction_to_the_Modeling_and_Analysis_of_Complex_Systems_(Sayama)/11%3A_Cellular_Automata_I_-_Modeling/11.05%3A_Examples_of_Biological_Cellular_Automata_Models.

Shishikura, Mitsuhiro. "The Hausdorff Dimension of the Boundary of the Mandelbrot Set and Julia Sets." *Annals of Mathematics* (Mathematics Department, Princeton University) 147 (March 1998): 225-267.

Sood, Ishaan, Abhirakshit, and Asapu Shiva. "Phase Space Dynamics in Chua's Circuit." Project, IIT Kanpur, Kanpur, 2014, 5.

Springel, Volker. "Astronomers may have spotted strands in the 'cosmic web' linking galaxies." *Popular Science.* Max Planck Institute For Astrophysics. October 2019. https://www.popsci.com/cosmic-web-filament/ (accessed January 2020).

Strogatz, Steven H. *Nonlinear Dynamics and Chaos.* New York: Perseus Books, 1994.

Team, R Core. "R: A Language and Environment for Statistical Computing." Vienna: R Foundation for Statistical Computing, 5 July 2019.

Wikipedia. *Compartmental models in epidemiology.* https://en.wikipedia.org/wiki/Compartmental_models_in_epidemiology

yyz1335. *The Genesis wave.* 9 Oct 2008. www.youtube.com/watch?v=NM1r37zIBOQ